RSC Advances

ROYAL SOCIETY OF CHEMISTRY

www.rsc.org/advances

Journal Name

ARTICLE

The energy consumption and pellets' characteristics in the co-pelletization of oil cake and sawdust

Received 00th January 20xx,
Accepted 00th January 20xx

DOI: 10.1039/x0xx00000x

www.rsc.org/

Z. L. Huang[a], H. Li[a]*, X. Z Yuan[b], L. Lin[a,c]*, L. Cao[a,b], Z.H. Xiao[b], L.B. Jiang[b], C.Z. Li[a]

The improvement on the co-pelletization of biomass (cedarwood and camphorwood) and oil cake was carried out in the present work. The characteristics of raw materials were determined by chemical and physical analysis. The co-pelletization process was studied by quantifying the energy consumption of compaction and extrusion. The physical properties of pellets including moisture adsorption, pellet energy density and hardness were also determined. The blending of biomass with oil cake would increase the density of pellets, and thus reduce their costs during production, transport and storage. The energy consumption of compaction decreased with the increasing content of castor bean cake, while the energy consumption of extrusion and pellets' energy density had an opposite tendency. Moreover, the maximum compression force and hardness increased with the blend ratio of CAS (castor bean cake) rising. This thermal analysis suggests that adding CAS can enhance char combustion and lead to larger reactivity during char combustion. 10-20% of castor bean cake by mass would be a suitable proportion in the co-pelletization with biomass in terms of energy consumption and pellet properties.

Keywords: Oil cake; Pelletization; Energy consumption; Moisture absorption; Hardness; Combustion

1. Introduction

Biomass pellets have been considered as a high-quality fuel suitable for many industrial and residential applications [1,2]. The densities of pellets can be 4-10 times higher than those of sawdust or straw, which is helpful to reduce the costs of transport and storage [1,3]. However, the increasing price of raw material, limited adaptability of pellet unit and unsatisfying quality of pellets hinder the further development of pelletization industry [4]. Those challenges would be aggravated in some area accompanying with other biomass manufactures, such as biomass-power generation, paper making, and artificial boards etc. In East Asia, due to the competition for feedstock among several biomass industries, the price of raw material has climbed to 64-108 USD/t which is by far higher than that in Europe and North America. Major industrial enterprises in East Asia have to use various kinds of biomass with different shapes, including hard wood, soft wood and straw, so the dies and rollers in pellet unit have to be fed with different kinds/shapes of biomass, consequently shortening their operating life [5]. Therefore, several researches have been concentrating on the co-pelletization of mixture material [6-9].

The raw materials blends could contribute to the production of higher-quality pellets for combustion [6]. The biomass additives used in blending are usually bentonite, lignosulfonate, modified cellulose binders, proteins, etc [10,11]. The additives form a bridge, film or matrix to improve the pellet quality or minimize the variation of pellet quality [10-12]. However, the additives are more expensive than conventional biomass, which may affect the economic feasibility of biomass energy [11,13]. Therefore, the suitable additives should be chosen from solid waste or other byproducts.

Several researches of pelletizing additives focused on the identification of the combustion behaviour and the mechanical durability [14,15]. However, few works have been conducted to find a type of practical additives considering the optimization of energy consumption, pellet density, pellet hardness and moisture uptake.

In this study, castor bean cake, a kind of residue in the oil expression process, was utilized as the additive in the process of co-pelletization. On account of the biomass diversity in physical and chemical properties, the experiments were carried out to evaluate the effects of biomass types (softwood and hardwood) and the blending proportions of oil cake on the energy consumptions of pelletization and the pellets properties.

2. Materials and methods

2.1Materials

Woody sawdust of cedarwood (CED) and camphorwood (CAM) used in this work were selected as raw materials, representing softwood and hardwood respectively. The selected Oil cake was castor bean cake (CAS), which is obtained from the castor bean expression process in a pilot of Hunan Academy of Forestry

[a] Institute of Biological and Environmental Engineering, Hunan Academy of Forestry, Changsha 410004, P.R. China.
[b] College of Environmental Science and Engineering, Hunan University, Changsha 410082, P.R. China.
[c] School of Food and Biological Engineering, Jiangsu University, Zhenjiang 212013, P.R.China.

(Changsha, China). Proximate analysis was carried out according to the Standard Practice for the Proximate Analysis of Coal and Coke (GB/T212-2001) using a Vario EL III elemental analyzer (Germany). Three replicates were measured for each raw material. The characteristics of those raw materials are presented in Table 1.

The raw materials were dried by air (40 ^{o}C, 48 h), ground by pulverizer and then screened into fractions of particle size below 0.45 mm. The average sawdust moisture content was 5% after dry. The moisture content of feedstock was adjusted to 10% by adding with deionized water, and then the feedstock was maintained in plastic bottles at 4 ^{o}C for 48 h to mix them uniformly.

2.2. Pelletizing process and characteristics analysis

As shown in Fig.1, ADWD-10, a piston-cylinder unit installed with a punch and die set, was used for pelletization. A die set of 7 mm inside diameter and 120 mm length with a piston of 6.8 mm in diameter and 80 mm in length was installed for making a single pellet. The die was encircled with a heating tap connecting to a temperature controller to preheat the cylinder, simulating the heat generated in the industrial pelletization [16]. A removable plug was used to plug the end of the die. The transducer was applied to measure the compression force and displacement during pelletization and the data was recorded by a computer.

CAS was added into CED and CAM with the proportions of 0%, 5%, 10%, 15%, 20%, and 25%, respectively. Prior to the pelletization, the die set was heated up to 110 ^{o}C. The prepared material was loaded in DWD-10 at the same dosage, with the top hole of the die set filled with approximately 0.8 g of prepared sample. The loaded sample was compressed at a rate of 2 mm/min until the desired pressure was achieved. The compaction rod was applied a maximum force of 4000 N and held for 30 s. After then, the pellet was extruded from the die set and cooled down immediately. Seven pellets were made for each sample, measured in length and weight and kept in plastic bottles for two weeks.

2.3 Moisture absorption

The pellets for each blended sample were dried at 105 ^{o}C for 48 h before moisture absorption test. That test were carried out in a humidity chamber (30 ^{o}C and 90% relative humidity).The weight of the pellets were determined with the intervals of 20 min in the first five hours. After then, the final moisture absorption was measured after 2 days. The kinetics of moisture absorption is presented by using the ASABE formulation as following [14,17]

$$M\text{-}M_e/M_i\text{-}M_e=e^{-k\,t} \quad (1)$$

Where M is the instantaneous moisture content (decimal, dry basis), M_e is the equilibrium moisture content (decimal, dry basis), and M_i is the initial moisture content (decimal, dry basis). The coefficient k is an absorption constant (min^{-1}), and t is the exposure time (min).

2.4 Mechanical hardness

The analysis of pellet mechanical hardness was carried out by the ADWD-10 pressure unit. The stored pellets were horizontally placed at a flat surface under the compression bar. The pressure force was loaded at the centre of the pellet. The compression bar was run at a certain rate of 2 mm/min until the pellet was broken, in which the collapse force reach the maximum pressure. The collapse force and corresponded distances were recorded by a computer. Three replicates were conducted for each sample. The Meyer hardness was calculated using the following equation [18]:

$$MH=F/[\pi(Dh\text{-}h^2)] \quad (2)$$

Where MH is Meyer hardness (N/mm^2); F is maximum pressure (N); D is pellet diameter (mm) and h is the corresponded indentation depth of maximum pressure (mm).

2.5 Thermogravimetric analysis (TG)

Thermogravimetric analysis was performed using a TG-60 analyzer (JAP) for evaluating combustion characteristic of materials. In this study, the temperature program consisted of two steps: from room temperature to 105 ^{o}C at 10 ^{o}C min^{-1} heating rate, and rising up to 800 ^{o}C at 15 ^{o}C min^{-1} heating rate. Air was used as purging gas at a flow rate of 100 mL/min. Mass between 3 and 5 mg of each sample was used to evaluate combustion behaviour, in order to reduce the interference of mass and heat on the test.

3. Results and discussion

3.1 Energy consumption

It was reported by a previous research that the processing of hardwood sawdust consumed more energy than softwood sawdust [19]. However, as shown in Fig. 2a and b, the opposite results were shown in the present work. Error bars in the figures represent standard deviations of seven replicates, which indicate the heterogeneous character of wood powder in the mechanical properties. The energy consumptions were 19.6 kJ/kg and 15.6 kJ/kg for CED and CAM, respectively. There are two explanations for that opposite result on the micro and macro views. On the micro view, the hemicellulose content in CAM is higher than that in CED (Table 1). The hemicellulose can act as a viscoelastic interface in lignocellulose's structure as the larger quantity of hydrogen boding in hemicelluloses [17]. The CAM with higher hemicellulose content consequently has a stronger tenacity with higher modulus of elasticity in the elastic region [17]. The higher tenacity of sawdust contributed to a lower energy consumption during the compaction [1]. As a result, lower energy is thus required during compaction process for CAM than CED. Meanwhile, on the macro view, higher energy consumption means higher friction consumption during pelletization. In Fig. 3a1-3, more intertwined fibers were identified on the surface of CED compared with the flat surface of CAM. The friction between CED particles was hence increased due to the large contact area in the intertwined fibers, resulting in higher compaction energy consumption for CED runs.

In Fig. 2a, lower compaction energy consumptions were applied with the CAS content increased for CED, while no significant change was observed for CAM. This can be due to the different fiber structures between CED and CAM [20]. The lubricating function of CAS was utilized in the intertwined fiber structure of CED, compared with no clear evidence in the flat structure of CAM. The CAS was squeezed into the gaps and voids between biomass particles, and consequently coated on the intertwined fiber surface of CED with residual oil, proteins and starch which can act as lubricant, resulting in the decline of the friction [8]. Meanwhile, the lower extrusion energy consumptions were obtained in all CED-CAS runs, while the extrusion energy consumption increased with CAS content rising in CAM-CAS runs (shown in Fig. 2b). The denatured proteins and gelatinized starch in CAS immobilized in the fiber matrix of CED contributed to the enhancement of hydrogen bonding and "solid bridge" among particles, leading to the improvement of pellets' plasticity, which can reduce the extrusion energy consumption [1]. Moreover, higher extrusion energy consumption was obtained with the increase of CAS content in CAM-CAS runs (Fig. 2b). This may be due to the viscidity of protein and starch in CAS during pelletization [17]. In the compaction process, several denatured proteins and gelatinized starch in CAS

were softened, and subsequently were squeezed into the space between pellet and inner wall of die as the flat surfaces of CAM particles lacks fiber matrix. The protein and starch were plasticized and adhered to the surface of inner wall of die, resulting in the higher friction during extrusion. Furthermore, the higher ash content in CAS was another reason for the higher friction (Table 1). Therefore, the extrusion energy consumption in CAM-CAS run increased with the increment of CAS content.

Furthermore, as shown in Fig. 2, the variations of compaction and extrusion energy consumption between CED-CAS and CAM-CAS were "narrowed" with CAS content at 10-20%. In industrial utilization, the limited feedstock species were more suitable for specific pelletization equipment as the variations of physical and chemical characteristics of biomass. The properties of mixing material can be uniformed by the addition of CAS, resulting in the homogeneous energy consumption and the increment of equipment service life [21].

3.2 Pellets density

In Table 2, the diameter and length resiliency for all pellets were approximate, indicating that the pure and blending pellets had good dimensional stability during storage. However, those results were distinguished with a previous research [22]. In previous work, the resiliency mainly occurred at the length direction with a decrease from 25% to 10% with the increase content of waste wrapping paper during storage [22]. The interlocking bonds in pellets were strengthened by additives, contributing to the increasing resistance of disruptive force and the reduction of length resiliency [9,22]. In the present study, the additive of CAS can also strengthen the interlocking bonds as the function of waste wrapping paper. Those differences may be due to the higher compression force in this study, leading to the stronger interlocking bonds in more stable matrix of CAS and biomass to resist the disruptive force [6,9,16].

No significant changes on the mass density were observed for the pellets after 20 days' storage, implying that the length resiliency can significantly affect the mass density of pellets during storage. However, the mass densities of CED-CAS and CAM-CAS increased with the increasing CAS content (Table 2). Such trends of pellet density were mainly due to the soften protein and starch flowing into the voids and gaps between biomass particles and forming tighter structures as shown in Fig. 3b1-3 and 3c1-3. The energy density of CED-CAS and CAM-CAS increased from 21.45 GJ/m^3 to 21.97 GJ/m^3 and 19.33 GJ/m^3 to 20.83 GJ/m^3, respectively. These results indicate that the CAS blended with biomass can improve the energy-quality of pellets in industrial application.

3.3 Moisture adsorption

The adsorption of moisture can "loose" the hydrogen bonding and solid bridge within pellets [16,23]. Dusts and fines were thus produced from the moisture uptake, causing the ignition and explosion during handling, storage and transportation [24]. In Fig. 4 and Table 3, the estimates for adsorptions rates (in first five hours) were 0.00442 min^{-1} and 0.00492 min^{-1} for CED and CAM, respectively. The higher hemicellulose content in CAM may cause the higher adsorptions rate in CAM. In addition, the closer structure of CED with compressed fibers resisted the moisture uptake compared with CAM. However, the equilibrium moisture adsorption (measured in the 48th hour) was 13.10% for CED and 11.63% for CAM. These results indicate that the intertwined fiber structure of CED can provide more sites to absorb moisture compared to that of CAM. Moreover, there was no clear variations for CED-CAS and CAM-CAS with the increasing of CAS content in terms of the moisture adsorption.

3.4 Mechanical hardness

It can be depicted in Fig. 5 that the maximum collapsing force and Meyer hardness of CED were significantly higher than those of CAM. This may attribute to the diversity of particle structures mentioned in Section 3.1. As shown in Fig. 3a1-3, more intertwined fibers were identified on the surface of CED compared with the flat surface of CAM. The fiber matrix and solid bridge between CED particles were hence strengthened due to the large contact area in the intertwined fibers, resulting in higher maximum collapsing force and Meyer hardness for CED runs. Meanwhile, in Fig. 5， the average maximum collapsing forces of CED-CAS and CAM-CAS increased from 63 N to 100 N and from 23 N to 53 N with the increasingly higher CAS content, respectively. It can be implied that the binders between particles were enhanced by the CAS due to the adhesive function of proteins and starch in CAS [9,22]. This is consistent with a previous research [25]. It was reported that the collapsing forces of alfalfa pellets which contained 17.6% and 22% protein were 425 N and 507 N, respectively [25]. However, there were difference trends on Meyer hardness between CED-CAS and CAM-CAS with CAS content increased. In Fig. 5a, the Meyer hardness of CAM-CAS increased from 3.93 N/mm^2 to 6.52 N/mm^2. This may due to the enhancement of hydrogen bonding and solid bridge with the addition of CAS [3,23]. However, a slight decline was detected for the Meyer hardness of CED-CAS in the range of 5.09-5.67 N/mm^2 with the CAS content increasing from 5% to 15%.

The Meyer hardness is determined by the maximum of collapsing force versus distance during compression, reflecting the resistance to deformation. As shown in Fig.6a, the distance of indentation depth increased at the same compression force with the increasing CAS content for CED, while an opposite tend was observed for CAM. Therefore, lower Meyer hardness was obtained at the CAS content of 10% and 15% in CED-CAS runs. On the micro level, the protein and starch contained in CAS, which was softened and acted as interlocking binder between biomass particles, can increase the elasticity of pellets matrix, resulting in the lower resistance to deformation [9,23]. In addition, the Meyer hardness in CED-CAS runs was enhanced slightly and leveled off around 5.2 N/mm^2 with the increase of CAS content from 15% to 25%. The further increase of maximum collapsing force contributed to the slight increase of Meyer hardness. However, the further increase of Meyer hardness couldn't be achieved due to the resistance to deformation of pellet, which can be confirmed by the images in Fig. 6a.

3.5 Combustion characteristic

It is evident from TG and DTG curves shown in Fig. 7 that the two types of biomass (CED and CAM) depicted three step weight losses: moisture evaporation, oxidative degradation and char combustion. The combustion parameters were characterized by ignition temperature, maximum DTG and temperature at maximum DTG summarized in Table 4. The higher maximum DTG in the DTG curves (Fig. 7 and Table 4) represent the strongly oxidative pyrolysis region and the temperature at maximum DTG is considered as a standard of the reactivity of materials [26]. The initial weight loss is attributed to the dehydration in samples at the temperature of 25-100 ^{o}C. In the region of oxidative degradation, the ignition temperatures were 223-214 ^{o}C and 222-211 ^{o}C for CED and CAM sequences, respectively. The lower ignition temperature is due to

the residual oil in CAS which can act as the comburent during combustion. It was also found that the maximum DTG value decreased from 1.25 to 0.97 s^{-1} and from 1.12 to 0.47 s^{-1} for CED and CAM with the increasing content of CAS, respectively. This results indicated that high fixed carbon content (19.82%) and ash content (8.14%) in CAS can slow down the releasing and burning of combustible in biomass by covering the volatile matter. Furthermore, the close-knit structure formed by CAS may reduce the release level of volatiles [9]. As shown in Fig. 7, there is a increase in the maximum DTG in char combustion region with the increment of CAS content for both biomass materials. It was reported that char combustion could be improved by adding coal which can lead to higher HHV and stable combustion [27]. This result suggested that adding CAS can enhance char combustion and lead to larger reactivity during char combustion. It can be explained by two reasons as follows: firstly, the higher fixed carbon content in CAS can improve the char combustion compared with that in biomass. Besides, the char combustion rate can be enhanced by mutual interaction caused by adding CAS. As a result, the addition of CAS has the similar function with coal in terms of combustion.

Conclusions

There is a significant decrease in the compaction energy consumption for biomass with the increasing content of CAS. Furthermore, the denaturation of protein in CAS during compression can improve the formation of solid bridge and hydrogen bonding among particles, resulting in increasingly higher maximum compression force or Meyer hardness of pellets. Moreover, the addition of CAS can enhance char combustion, which led to larger reactivity during char combustion. However, due to the low output and the higher ash content in CAS, this additive should be added in a relatively low proportion of 10-20% by mass, which can be suitable for pellet production. The oil cake, a kind of the residue obtained from the castor bean expression process, meets the requirement of economic feasibility and commercial production.

Acknowledgements

The authors gratefully acknowledge the financial support provided by the National Natural Science Foundation of China (No. 21407046, No. 31470594), and the Key Laboratory of Renewable Energy Chinese Academy of Sciences (No. y407k91001).

Notes and references

1 H. Li, X.H. Liu, R. Legros, X.T. Bi, C.J. Lim, S. Sokhansanj, *Applied Energy,* 2012, 93, 680-685.
2 Y.Z. Lu, C.W. Du, C.B Yu, J. Zhoua, *Analytical Methods,* 2014, 25, 86-91.
3 Z. Liu, A. Quek A, R. Balasubramanian, *Applied Energy,* 2014, 113, 1315-1322.
4 A. Pirraglia, R. Gonzalez, D. Saloni, J. Denig J, *Energy Conversion and Management,* 2013, 66, 153-164.
5 J. Berghel, S. Frodeson, K. Granström, R. Renström, M. Ståhl, D. Nordgren, P. Tomani, *Fuel Processing Technology,* 2013, 112, 64-69.
6 M.V. Gil, P. Oulego, M.D. Casal, C. Pevida, J.J. Pis, F. Rubiera, *Bioresource Technology*, 2010, 101, 8859-8867.
7 H. Li, L.B. Jiang, C.Z. Li, J. Liang, X.Z. Yuan, Z.H. Xiao, Z.H. Xiao, H. Wang, *Fuel Processing Technology,* 2015, 132, 55-61.
8 M. Ståhl, J. Berghel, *Biomass and Bioenergy.* 2011;35:4849-4854.
9 L. Jiang, J. Liang, X.Z. Yuan, H. Li, C.Z. Li, Z.H. Xiao, *Bioresource Technology,* 2014, 166, 435-443.
10 N. Kaliyan, R. Morey, *Biomass and Bioenergy,* 2009, 33, 337-359.
11 H.J. Ahn, H.S. Chang, S.M. Lee, D.H. Choi, S.T. Cho, G.S. Han, I. Yang, *Renewable Energy,* 2014, 62, 18-23.
12 W.H. Chen, W.Y. Cheng, K.M. Lu, Y.P. Huang, *Applied Energy,* 2011, 88, 3636-3644.
13 J. Chau, T. Sowlati, S. Sokhansanj, F. Preto, S. Melin, X.T. Bi, *Applied Energy,* 2009, 86, 616-621.
14 P.S. Lam, S. Sokhansanj, X.T. Bi, C.J. Lim, S.H. Larsson, *Bioresource Technology*, 2012, 116, 396-402.
15 D. Bergström, S. Israelsson, M. Öhman, S.A. Dahlqvist, R. Gref, C. Boman, *Fuel Processing Technology,* 2008, 89, 1324-1329.
16 P.Y. Lam, P.S. Lam, S. Sokhansanj, X.T. Bi, C.J. Lim, S. Melin, *Fuel,* 2014, 117, 1085-1092.
17 P.S. Lam, S. Sokhansanj, X.T. Bi, C.J. Lim, S. Melin, *Energy & Fuels,* 2011, 25, 1521-1528.
18 L. Tabil, S. Sokhansanj, W. Crerar, R. Patil, M. Khoshtaghaza, A. Opoku, *Canadian Biosystem Engineering,* 2002, 44, 55-63.
19 N.P.K. Nielsen, J.K. Holm, C. Felby, *Energy & Fuels,* 2009, 23, 3211-3216.
20 D.R. Morris, F.R. Steward, C.A. Gilmore, *Energy Conversion & Management,* 2000, 41, 1557-1568.
21 S. Patel, A.M. Kaushal, A.K. Bansal, *Pharmaceutical Research*, 2007, 24, 111-124.
22 L. J. Kong, S.H. Tian, C. He, C.M. Du, Y.T. Tu, Y. Xiong, *Applied Energy*, 2012, 98, 33-39.
23 N. Kaliyan, RV Morey, *Bioresource Technology*, 2010, 101, 1082-1090.
24 C. Serrano, E. Monedero, M. Lapuerta, H. Portero, *Fuel Processing Technology*, 2011, 92, 699-706.
25 L. Tabil, S. Sokhansanj, *Canadian Agricultural Engineering,* 1997, 39, 17-23.
26 Q. Yi, F. Qi, G. Cheng, Y. Zhang, B. Xiao, Hu Z, *Journal of Thermal Analysis and Calorimetry,* 2012, 112, 1475-1479.
27 C. Zhou , G. Liu, S. Cheng, T. Fang, P.K. Lam, *Bioresource Technology,* 2014, 166, 243-251.

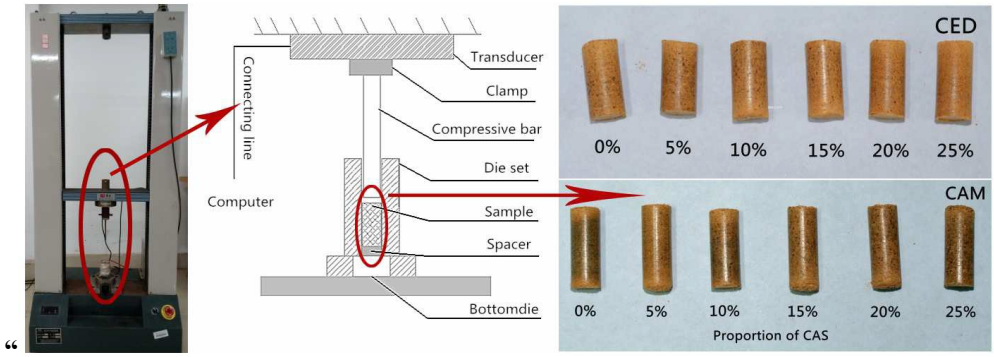

Fig.1. The pictures of pellet die setup: the ADWD-10 universal press, the schematic diagram of apparatus and the pellets.

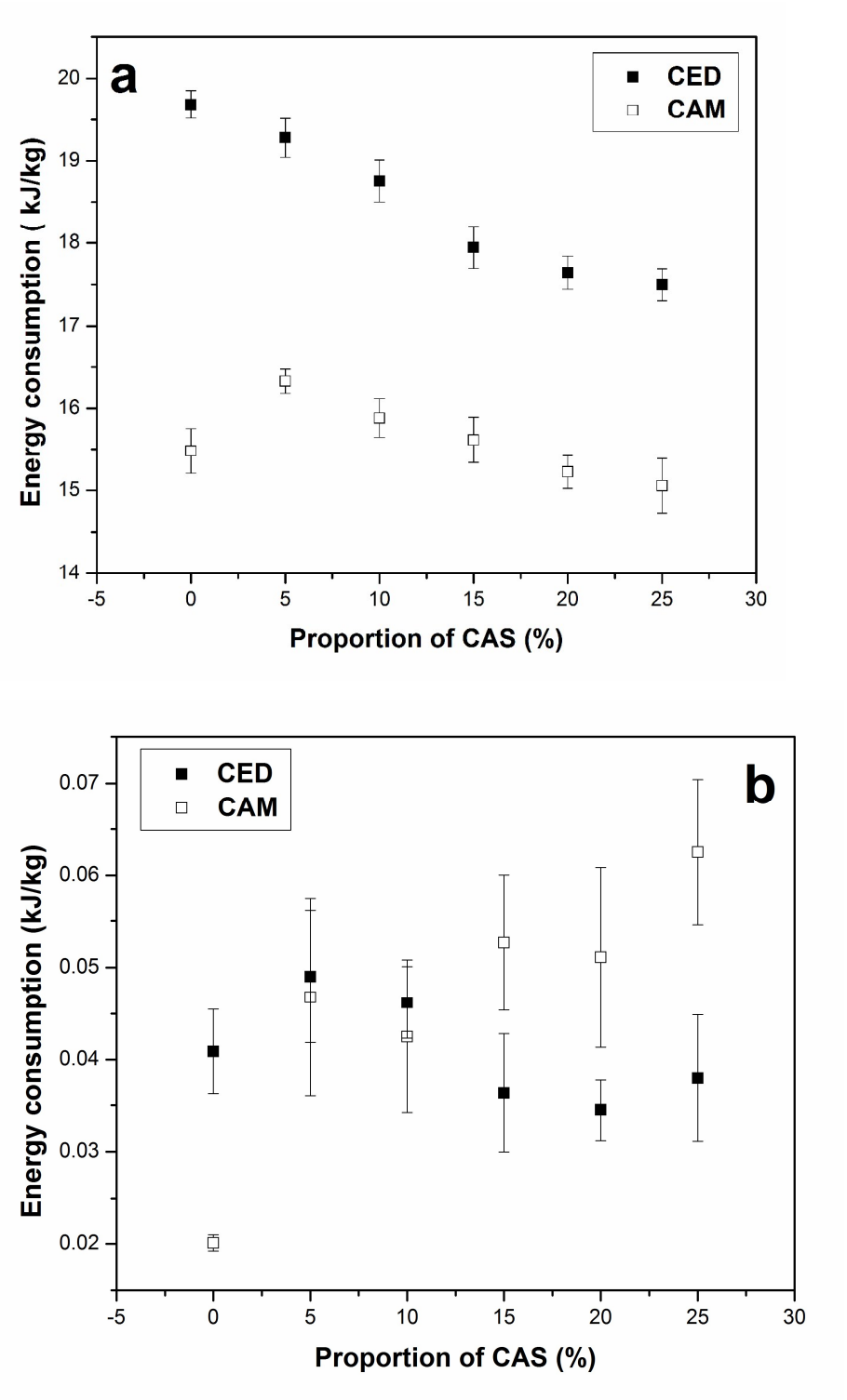

Fig. 2. The energy consumption of compression (a) and extrusion (b) as a function of content of CAS.

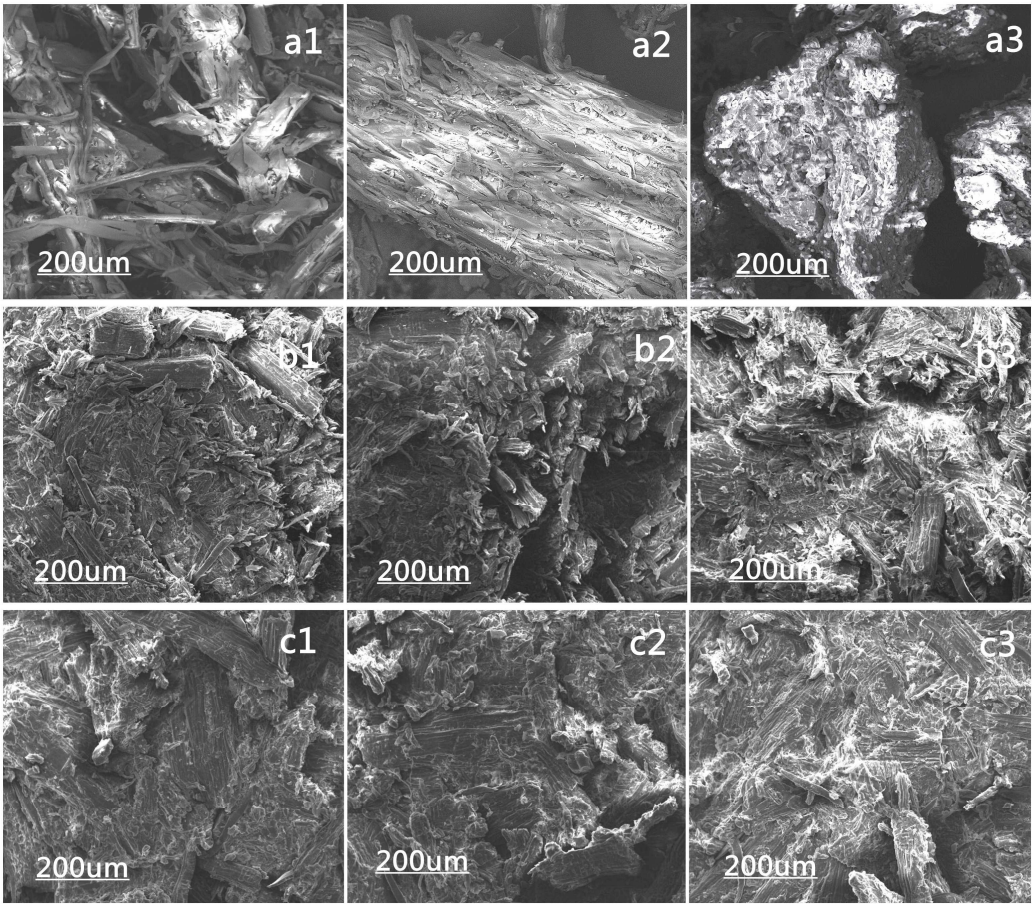

Fig.3. SEM micrographs of raw materials and pellets. (a1) raw CED; (a2) raw CAM; (a3) raw CAS; (b1) CED; (b2) 90% CED + 10% CAS; (b3) 75% CED + 25% CAS; (c1) CAM; (c2) 90% CAM + 10% CAS; (c3) 75% CAM + 25% CAS.

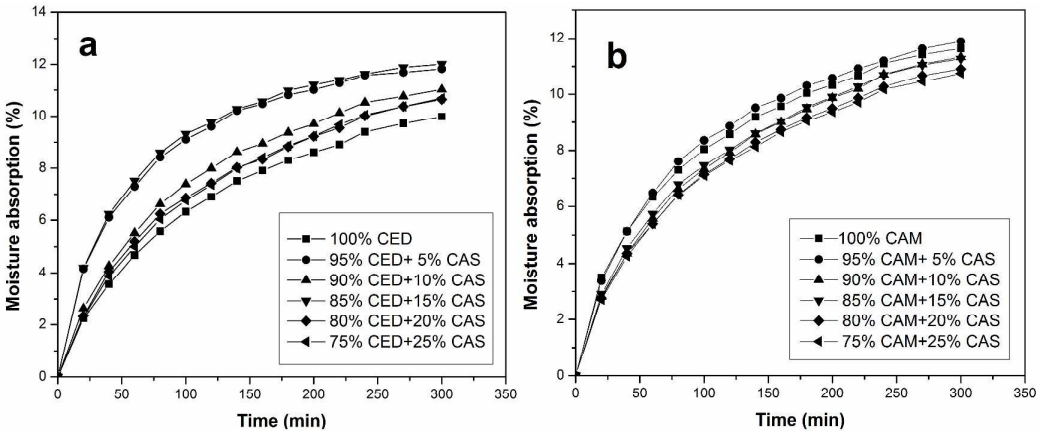

Fig. 4. the instantaneous moisture content of pellets densified from blends of biomass and CAS. (a) CED; (b) CAM

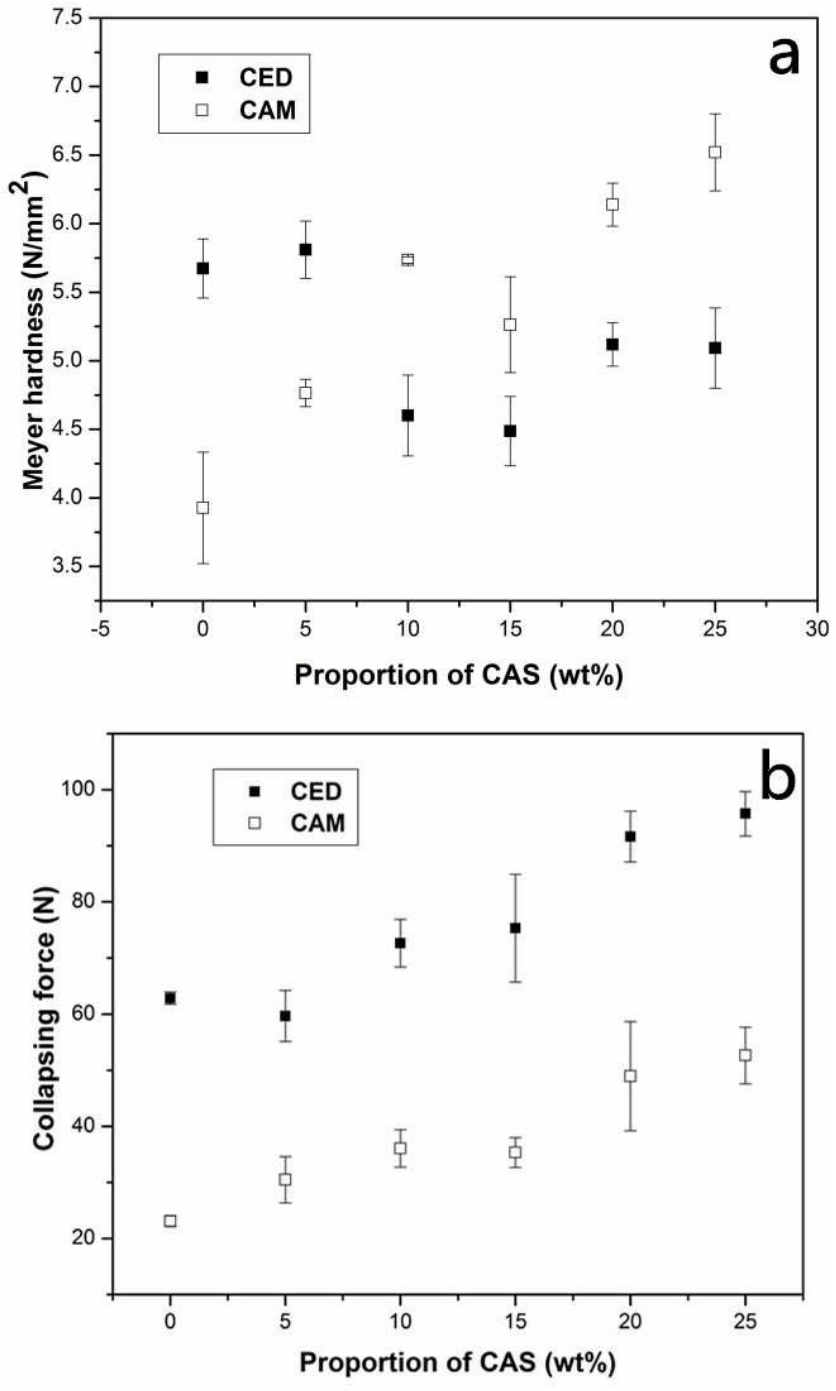

Fig. 5. Meyer hardness and the collapsing force of pellets as a function of content of CAS. (a) Meyer strength; (b) collapsing force.

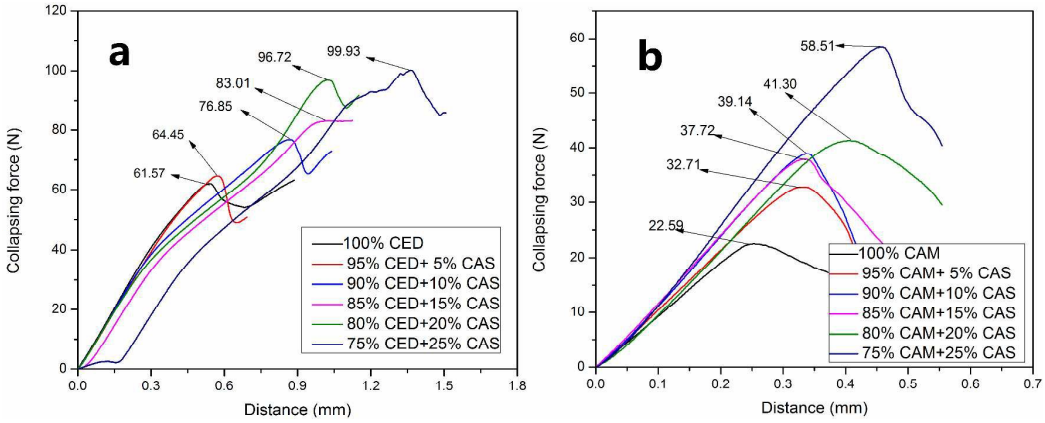

Fig. 6. Collapsing force versus distance graph of pellets as a function of content of CAS. (a) CED; (b) CAM.

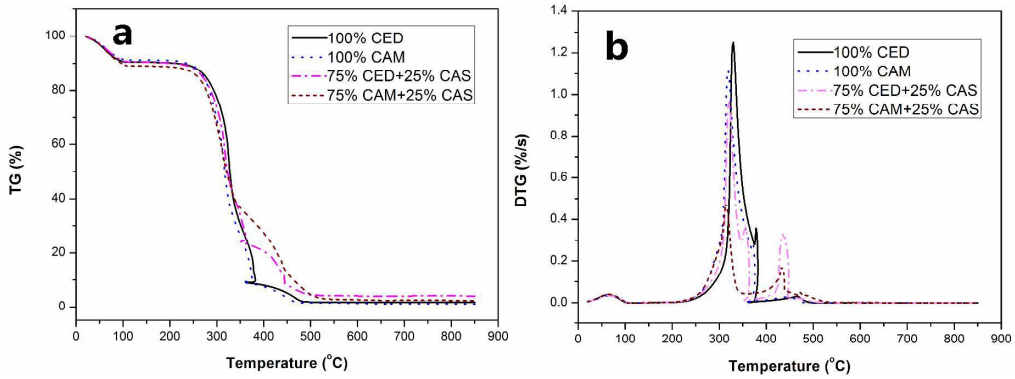

Fig.7. TG and DTG curves of raw and torrefied pellets in a nitrogen flow rate of 50 mL/min and a air flow rate of 100 mL/min at a heating rate of 15 °C/min. (a) TG; (b) DTG

Table 1

Chemical analysis of raw materials (wt.%. dry basis).

Analysis		Cedarwood	Camphorwood	Castor bean cake
Elemental analysis (%)[a]	C	48.95	48.18	44.21
	H	5.91	6.09	5.93
	O	44.49	45.03	41.38
	N	0.65	0.70	7.92
	S	---	---	0.56
Fiber analysis (%)	Hemicelluloses	12.05	20.82	28.98
	Cellulose	36.22	38.87	20.73
	Lignin	27.61	24.40	23.75
Proximate analysis (%)	Moisture	7.63	6.67	7.42
	Volatile matter	74.49	79.02	64.62
	Fixed carbon	16.68	12.53	19.82
	Ash	1.20	1.78	8.14
Protein analysis (%)		---	---	6.24

[a] Elemental analysis (dried and ash-free base)

Table 2

Mass and high heating values of raw materials.

Samples	Size (mm)[a]		Resiliency (mm)[b]		Mass density (kg/m^3)[a]		Mass density (kg/m^3)[b]		HHV (MJ/kg)	Energy density (GJ/m^3)
	Diameter	Length	Diameter	Length	Average	SD	Average	SD		
CED										
100%CED	7.45	15.48	0.10	0.72	1086.24	3.86	1095.89	4.81	19.57	21.45
95%CED+5%CAS	7.44	15.44	0.18	0.97	1088.04	7.74	1088.97	16.21	19.58	21.32
90%CED+10%CAS	7.43	15.25	0.10	0.89	1106.39	7.11	1112.63	5.87	19.48	21.67
85%CED+15%CAS	7.44	15.58	0.01	1.01	1095.91	14.38	1101.79	14.68	19.37	21.34
80%CED+20%CAS	7.44	15.22	0.18	1.09	1113.23	10.85	1124.60	13.97	19.35	21.76
75%CED+25%CAS	7.45	15.14	0.14	0.89	1122.31	10.78	1132.37	14.41	19.40	21.97
CAM										
100%CAM	7.46	21.04	0.02	0.34	1012.43	32.22	1025.15	30.67	18.86	19.33
95%CAM+5%CAS	7.46	20.99	0.04	0.95	1019.09	21.67	1026.58	6.16	18.89	19.39
90%CAM+10%CAS	7.43	20.03	0.04	0.62	1057.17	19.86	1075.01	22.32	19.05	20.48
85%CAM+15%CAS	7.44	20.65	0.01	0.42	1045.79	11.96	1061.04	8.87	18.87	20.02
80%CAM+20%CAS	7.44	19.97	0.01	0.42	1072.29	40.48	1085.91	35.50	19.08	20.72
75%CAM+25%CAS	7.44	19.87	0	0.80	1096.12	8.10	1098.66	8.93	18.96	20.83

a: Measured after removal

b: Measured after 20 days

Table 3

Data on moisture adsorption

Samples	CED			CAM		
	Equilibrium moisture adsorption	Absorption rate k (min^{-1})	R-Square	Equilibrium moisture adsorption	Absorption rate k (min^{-1})	R-Square
0% CAS	13.10	0.00442	0.98	11.63	0.00492	0.99
5% CAS	13.55	0.00601	0.96	11.88	0.00529	0.98
10% CAS	13.61	0.00511	0.98	11.32	0.00469	0.99
15% CAS	14.20	0.00526	0.95	11.27	0.00468	0.99
20% CAS	14.14	0.00422	0.98	10.90	0.00405	0.98
25% CAS	14.12	0.00436	0.98	10.75	0.00432	0.98

Table 4

Combustion characteristic of raw biomass, torrefied biomass and their blends with CAS.

Samples	Oxidative degradation			Char combustion		
	Temperature range (^{o}C)	T_{peak} (^{o}C)	Maximum DTG (% s^{-1})	Temperature range (^{o}C)	T_{peak} (^{o}C)	Maximum DTG (% s^{-1})
100%CED	221-375	330	1.25	375-493	465	0.03
95%CED+5%CAS	223-367	338	1.14	367-495	467	0.04
90%CED+10%CAS	220-361	335	1.19	361-499	462	0.06
85%CED+15%CAS	215-359	339	1.26	359-497	460	0.05
80%CED+20%CAS	222-360	336	1.19	360-507	459	0.25
75%CED+25%CAS	214-360	320	0.97	360-500	436	0.34
100%CAM	213-363	319	1.12	363-479	446	0.03
95%CAM+5%CAS	218-354	337	1.12	354-477	447	0.03
90%CAM+10%CAS	213-352	323	1.06	352-492	451	0.05
85%CAM+15%CAS	219-357	322	0.93	357-507	446	0.06
80%CAM+20%CAS	222-348	330	0.71	348-496	439	0.09
75%CAM+25%CAS	211-365	316	0.47	365-532	433	0.17

Graphical abstract

Schematic illustration of co-pelletization camphorwood with caster bean cake.